

in the B6C3F1 mouse liver suggests that a common mechanism of oncogene activation is occurring in tumor tissue. Such a common mechanism is predictable because of the high degree of genetic similarity characteristic of inbred strains. Notably, the C3H mouse (the paternal genetic contributor in the B6C3F1 hybrid cross) has an even higher incidence of spontaneous hepatocellular tumors than does the B6C3F1 mouse (4).

One possible mechanism accounting for both the high spontaneous tumor incidence in the B6C3F1 mouse and the observed high transforming activity could be germ line transmission of the oncogene, resulting in a genetic predisposition to neoplasia. To evaluate this possibility, we isolated DNA from nontumorous liver tissue from eight animals whose tumor DNA induced foci in the NIH 3T3 assay. This DNA was transfected into NIH 3T3 cells as before. An equal number of control cultures were treated with calf thymus DNA. After 3 weeks no foci were observed in any of the cultures.

Thus the cellular oncogene detected in the spontaneously occurring hepatocellular carcinomas is not attributable to germ line transmission. Similar results have been reported for human patients having familial syndromes associated with a greatly increased cancer risk (8). This suggests that the active cellular oncogene found in the spontaneous liver tumors arose from alterations in individual somatic cells. In addition, the observation that DNA from 9 of 11 tumor-bearing animals produced transforming activity implies that some factor predisposing to malignancy is genetically transmitted in this strain of mouse. These results indicate that the B6C3F1 mouse is dissimilar to the genetically diverse human population in its ability to activate, with a very high frequency, a specific tumor-associated oncogene.

The detection of a cellular oncogene in the B6C3F1 mouse liver provides the opportunity to address questions of significant toxicological interest. For example, several studies have shown an increase in the incidence of liver tumors in the B6C3F1 mouse after prolonged exposure to chemical agents. Many of these agents have demonstrated genotoxic activity (defined as a direct chemical interaction with DNA), and it is generally concluded that this enhancement occurs through a somatic mutational mechanism. However, increased incidences of hepatic tumors in the B6C3F1 mouse have also been observed after treatment with agents that appear to be nongenotoxic in nature but that increase cellular

proliferation (9–13). Such conflicting results create a considerable dilemma in interpreting bioassay results.

It is attractive to hypothesize that substances that increase tumor development by apparently increasing cellular proliferation do so by altering the quantitative or temporal expression of cellular oncogenes. Recent data from several laboratories have shown a quantitative increase in oncogene expression in response to proliferative stimuli (14–16). In addition, there is evidence associating quantitative changes in oncogene expression with tumor development (17–19). Whether similar changes are important in the increased induction of liver tumors in the B6C3F1 mouse after chemical exposure remains to be determined.

Detection of a cellular oncogene in the B6C3F1 liver might provide insight into the unusually high frequency of spontaneous tumors in this strain of mouse. An understanding of this process may have important implications for the interpretation of animal bioassay data and may provide for more informed estimates of risk from chemical exposure in humans.

TONY R. FOX

PHILIP G. WATANABE

*Mammalian and Environmental
Toxicology Research Laboratory,
Dow Chemical U.S.A.,
Midland, Michigan 48640*

References and Notes

1. K. C. Chu, C. Cueto, J. Ward, *J. Toxicol. Environ. Health* **8**, 251 (1981).
2. Interdisciplinary Panel on Carcinogenicity, *Science* **225**, 682 (1984).
3. Task Force of Past Presidents of the Society of Toxicology, *Fundam. Appl. Toxicol.* **2**, 101 (1982).
4. International Expert Advisory Committee to the Nutrition Foundation, *The Relevance of Mouse Liver Hepatoma to Human Carcinogenic Risk* (Nutrition Foundation, Inc., Washington, D.C., 1983).
5. S. Pulciani *et al.*, *Proc. Natl. Acad. Sci. U.S.A.* **79**, 2845 (1982).
6. A. Eva, S. R. Tronick, R. A. Gol, J. H. Pierce, S. A. Aaronson, *ibid.* **80**, 4926 (1983).
7. S. Pulciani *et al.*, *Nature (London)* **300**, 539 (1982).
8. S. W. Needleman, Y. Yuasa, S. Srivastava, S. A. Aaronson, *Science* **222**, 173 (1983).
9. F. F. Becker, *Cancer Res.* **42**, 3918 (1982).
10. National Cancer Institute, *DHEW Publ. 77-813* (1977).
11. National Cancer Institute, *Carcinogenesis Bioassay of Chloroform* (TID PB264018/AS, National Technical Information Service, Springfield, Va., 1976).
12. R. H. Reitz, T. R. Fox, J. F. Quast, *Environ. Health Perspect.* **46**, 163 (1982).
13. A. M. Schumann, J. F. Quast, P. G. Watanabe, *Toxicol. Appl. Pharmacol.* **55**, 207 (1980).
14. M. Goyette, C. J. Petropoulos, P. R. Shank, N. Fausto, *Science* **219**, 510 (1983).
15. K. Kelly, B. H. Cochran, C. D. Stiles, P. Leder, *Cell* **35**, 603 (1983).
16. J. Campisi, H. E. Gray, A. B. Pardee, M. Dean, G. E. Sonenshein, *ibid.* **36**, 241 (1984).
17. M. Schwab, K. Alitalo, H. E. Varmus, J. M. Bishop, D. George, *Nature (London)* **303**, 497 (1983).
18. K. Alitalo, M. Schwab, C. C. Lin, H. E. Varmus, J. M. Bishop, *Proc. Natl. Acad. Sci. U.S.A.* **80**, 1707 (1983).
19. D. Kozbor and C. M. Croce, *Cancer Res.* **44**, 438 (1984).
20. We thank R. Weinberg for providing the NIH 3T3 cells and M. Barbacid, J. McCormick, R. Reitz, J. Saunders, and A. Schumann for their helpful discussion.

22 October 1984; accepted 18 December 1984

Brain Dopamine and Serotonin Receptor Sites Revealed by Digital Subtraction Autoradiography

Abstract. *Autoradiography combined with image analysis permitted quantitative visualization of dopamine (D₂) and serotonin (S₂) binding sites in rat brain. Forebrain sections were incubated with tritiated spiroperidol alone or with tritiated spiroperidol plus unlabeled compounds that saturated the D₂ or S₂ sites. By subtracting the digitized image of an autoradiograph derived from the latter sections from that of the former, the D₂ or S₂ sites were specifically revealed. The resulting quantitative images demonstrate the differing anatomical distributions of these sites. The D₂ site is largely restricted to the striatal complex (caudate-putamen, nucleus accumbens septi, and olfactory tubercle), whereas the S₂ site is enriched in layer 5 of motor cortex, the perirhinal and cingulate cortices, and the claustrum.*

The action of dopamine in the forebrain of humans and other mammals has been linked to such diverse functions as sensorimotor coordination, affect, and cognition (1). Because dopamine seems to modulate sensorimotor functions and cognitive processes through its interaction with the D₂ class of dopamine receptors (2), anatomically distinct populations of D₂ receptors are likely to subservise these specific dopamine-dependent behaviors. When brain sections are incubated with radioligands that bind with high affinity to the D₂ receptor, the

resulting autoradiographs can reveal the distribution of these sites in the forebrain with high resolution (3, 4). In this report we describe the use of computer-based imaging techniques to analyze [³H]spiroperidol autoradiographs and provide what appears to be the first quantitative visualization of D₂ and serotonin S₂ sites in the mammalian forebrain.

Tritiated spiroperidol labels both D₂ and S₂ sites with nanomolar affinities in brain homogenates or thin sections (3–6). The [³H]spiroperidol binding to these two sites is distinguished by using unlabeled

beled ligands that compete for one site or the other. The [^3H]spiroperidol bound in the presence of the competitor for the D_2 or S_2 site is subtracted from the total [^3H]spiroperidol bound to determine, respectively, the dopaminergic or serotonergic component. Although this subtraction approach has been used widely to distinguish receptor types in brain homogenates, it has not, to our knowledge, previously been applied to autoradiographic images. Adjacent brain sections were incubated with [^3H]spiroperidol alone or in combination with unlabeled compounds that selectively occupy the D_2 or S_2 sites. Digitized computer images of the latter sections were superimposed on and subtracted from the former to derive quantitative "difference im-

ages" of the D_2 and S_2 sites, respectively.

Consecutive 20- μm -thick coronal sections were collected from rat forebrain blocks located 7.5 to 9.5 mm anterior to the interaural line (7). The sections were thaw-mounted onto gelatin-coated slides and incubated for 5 minutes at 22°C in tris buffer plus ions and for 30 minutes at 36°C in the same buffer that contained [^3H]spiroperidol (25.0 to 31.7 Ci/mmol; New England Nuclear) with or without various concentrations of unlabeled displacer compounds (8). Unlabeled ligands included the D_2 receptor antagonist (-)-sulpiride (9-11), the S_2 receptor antagonist ketanserin (Janssen R 41468 (12, 13), or (+)-butaclamol, which displaces [^3H]spiroperidol from D_2 and S_2 sites (6,

10, 11, 13, 14). After the incubation the sections were given three 1-second rinses in buffer at 0°C, dried at room temperature, and apposed for 3 weeks to tritium-sensitive film [LKB (^3H)-Ultrafilm] along with ten 20- μm -thick brain paste standards containing various concentrations of [^3H]formaldehyde. The autoradiographic negatives were developed for 5 minutes in Kodak D-19.

The illuminated image of each autoradiograph was collected by a video camera. An image array processor (DeAnza Systems model IP 5500) converted the analog video signal to a digital display composed of 512 by 480 picture elements (pixels), each with a gray value ranging from 0 to 255 (15). Because of nonlinearities in the film and image array proces-

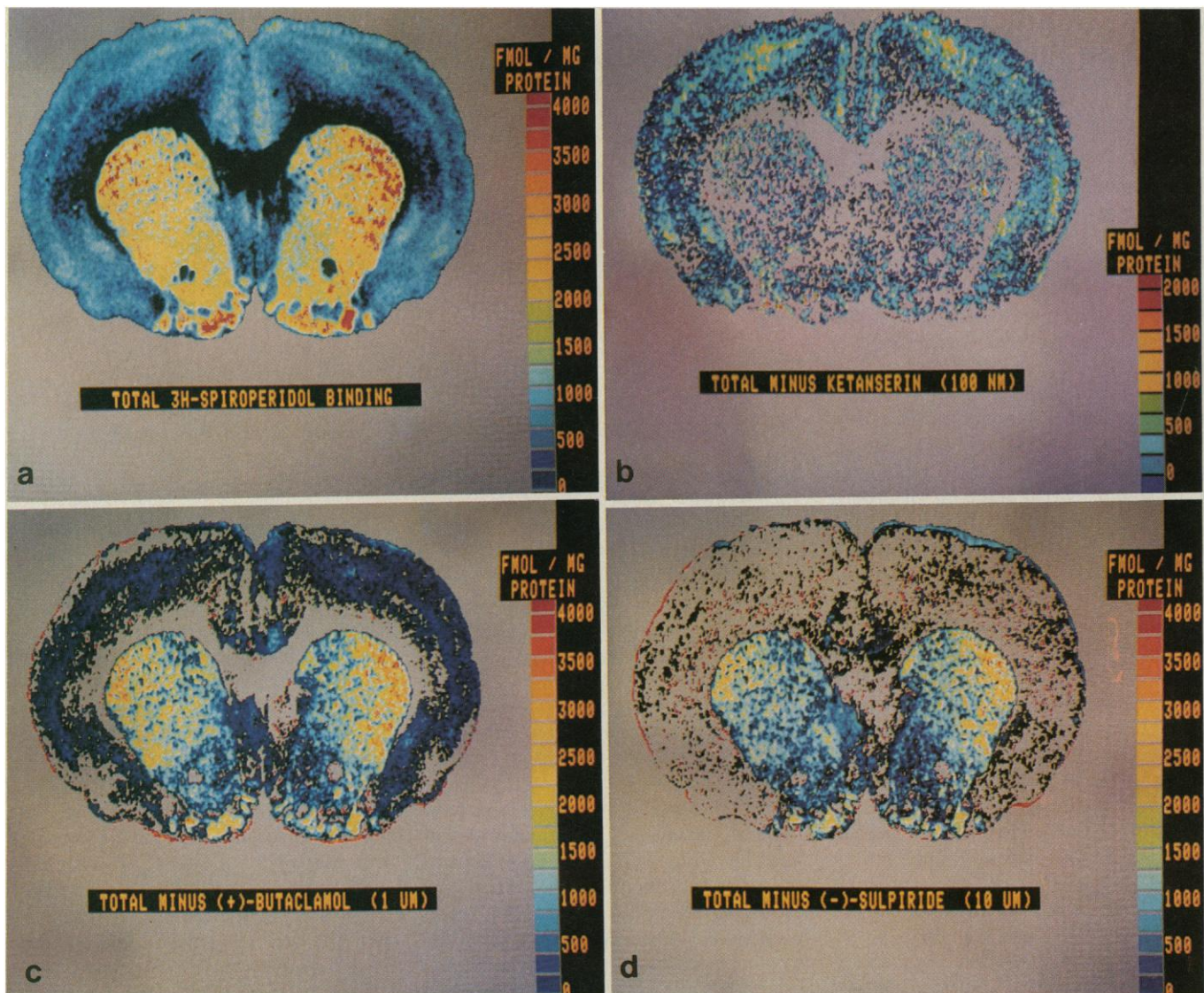


Fig. 1. (a) Color-coded image of [^3H]spiroperidol (1.3 nM) binding to a representative coronal forebrain section in the absence of displacer (total binding). (b, c, and d) Difference images that depict [^3H]spiroperidol binding to sites displaced by 1 μM (+)-butaclamol (b), 100 nM ketanserin (c), or 10 μM (-)-sulpiride (d). The images in (b) to (d) were produced by subtracting the linearized gray values of image pixels of a section incubated in the presence of displacer from the superimposed image of total binding to a neighboring section. All pixels that surrounded each section or that represented zero or negative [^3H]spiroperidol concentrations after image subtraction were assigned an intermediate monochromatic gray value. The relation between perceived color and [^3H]spiroperidol concentration is depicted by the color scale to the right of each linearized brain section. The protein content of the brain mash standards was determined by the method of Bradford (24).

sor, these original gray values were not a linear function of [³H]spiroperidol concentration. However, by using the standard curve for each piece of film (that is, the function that relates tritium concentration to gray value), the original gray values in each brain image were transformed so that the new gray value of each pixel in the image was a linear function of the quantity of [³H]spiroperidol in that pixel ("linearization") (15).

Figure 1a shows the distribution of the total [³H]spiroperidol bound to a representative coronal section. Because this color-coded image represents tritium concentration as a linear function of the scale of 0 to 255, quantitative estimates of local [³H]spiroperidol concentration can be made by visually comparing individual brain regions to the color-coded scale (16). The highest total [³H]spiroperidol binding occurred in the olfactory tubercle, caudate-putamen, and nucleus accumbens septi. Moderately high binding was present in layer 5A of the motor cortex, the claustrum, and the cingulate and perirhinal cortices. Lesser concentrations of ligand were associated with layer 1 of the cerebral cortex, while very little [³H]spiroperidol labeled the anterior commissure, corpus callosum, or internal capsule fibers that perforate the caudate-putamen.

Displacement by unlabeled compounds of [³H]spiroperidol binding in five forebrain regions is shown in Fig. 2. Unlabeled (+)-butaclamol (Fig. 2A) displaced a significant proportion of the total [³H]spiroperidol binding in the nucleus accumbens septi, claustrum, olfactory tubercle, layer 5A of cerebral cortex, and caudate-putamen, with maximal effects occurring at 1 to 10 μ M (+)-butaclamol. In contrast, (-)-sulpiride displaced [³H]spiroperidol from the caudate-putamen, nucleus accumbens septi, and olfactory tubercle but failed at any concentration to displace the radioligand from layer 5A of the cerebral cortex or the claustrum (Fig. 2B). Finally, nanomolar concentrations of ketanserin showed the opposite pattern, displacing the majority of [³H]spiroperidol binding in the claustrum and layer 5A but none in nucleus accumbens septi, olfactory tubercle, or caudate-putamen (Fig. 2C) (17).

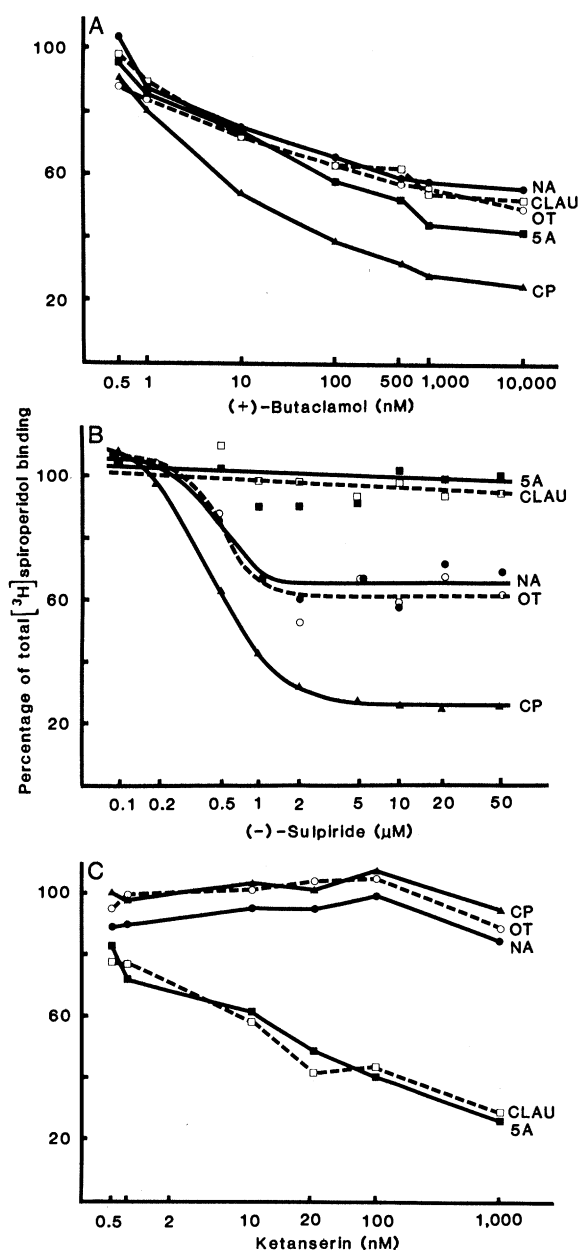
Because the image analysis system described here can digitize and linearize tritiated ligand binding autoradiographs, the image of a section incubated with [³H]spiroperidol plus a competitive displacer could be subtracted from a superimposed image of the total [³H]spiroperidol binding in a neighboring section to produce a quantitative difference image

that represents the binding that is displaced by that competitor. Difference images depicting the anatomical distribution of the 1 μ M (+)-butaclamol-displaced sites (D₂ and S₂), 100 nM ketanserin-displaced sites (S₂), and 10 μ M (-)-sulpiride-displaced sites (D₂) are shown in Fig. 1, b, c, and d, respectively.

Prior kinetic or equilibrium analyses of [³H]spiroperidol binding to rat forebrain revealed that (+)-butaclamol-displaceable binding is saturable, of nanomolar affinity, and consists of pharmacologically distinct S₂ and D₂ receptor sites (3, 4, 6, 10, 11, 13, 14). The present results, obtained with computer-assisted imaging techniques, indicate that, at the rostro-caudal level examined, the D₂ sites defined with (-)-sulpiride are restricted to the striatal complex (caudate-putamen,

nucleus accumbens septi, and olfactory tubercle), whereas the S₂ sites defined with ketanserin are located in the cerebral cortex and claustrum. Additional experiments with the dopamine receptor agonist 2-amino-6,7-dihydroxy-1,2,3,4-tetrahydronaphthalene also failed to detect a cortical D₂ component of [³H]spiroperidol binding in tissue sections at the level of the striatum or as far rostrally as the pole of the frontal cortex. This finding agrees with previous reports that the frontal cortex contains few if any D₂ sites (3, 11, 18), but conflicts with other studies indicating that 20 to 25 percent of the specific [³H]spiroperidol binding in frontal cortex homogenates has D₂ characteristics (10, 14). Quantitative autoradiographic studies from this laboratory have also identified a ketanserin-displaced component of [³H]spiroperidol

Fig. 2. Displacement of [³H]spiroperidol binding (1.3 to 1.6 nM) from the lateral caudate-putamen (CP), olfactory tubercle (OT), medial nucleus accumbens septi (NA), claustrum (CLAU), or layer 5A of the motor cortex (5A) by various concentrations of (+)-butaclamol (A), (-)-sulpiride (B), or ketanserin (C). The concentration of spiroperidol chosen (1.3 to 1.6 nM) was high enough to significantly label both D₂ and S₂ sites (16) yet low enough to yield high ratios of specific to nonspecific binding in the autoradiographs. A joystick-controlled rectangular cursor of variable size was positioned over the region of interest in the linearized image to compute the mean [³H]spiroperidol concentration in the region (15). Values for total [³H]spiroperidol bound are as follows (femtomoles per milligram of protein; means \pm standard errors for all nine brains used; four to six determinations per brain; two to four brains per displacer): lateral caudate-putamen, 2728 \pm 480; olfactory tubercle, 2972 \pm 517; nucleus accumbens, 2097 \pm 285; claustrum, 1402 \pm 216; and layer 5A, 1541 \pm 215. The following median inhibition constants ($K_{0.5}$ in nanomolar) were calculated: for (+)-butaclamol, 1.06 (caudate-putamen), 0.23 (olfactory tubercle), 0.93 (nucleus accumbens), 3.56 (layer 5A), and 1.77 (claustrum); for (-)-sulpiride, 92.5 (caudate-putamen), 14.4 (olfactory tubercle), and 26.0 (nucleus accumbens); and for ketanserin, 7.33 (layer 5A) and 1.03 (claustrum).



binding in the caudal (peripallidal) striatum, a finding that probably explains the small component (10 to 25 percent) of [³H]spiroperidol binding in striatal homogenates that has S₂ characteristics (10, 11, 18, 19).

The quantification afforded by digital subtraction autoradiography also allows comparisons to be made between the distribution of pharmacologically defined receptors and the density of their afferent innervation. For example, the striatal complex contains the most dense dopaminergic input of the forebrain as well as the highest concentration of D₂ sites. However, the enrichment of D₂ sites in the lateral caudate-putamen relative to the medial periventricular zone is unexpected. The sharp lateral-to-medial gradient in striatal D₂ density does not appear to be matched by any discernible parallel gradient in dopamine concentration (20). Also, the restricted laminar distribution of neocortical S₂ sites contrasts with the more scattered distribution of serotonergic axon terminals throughout the superficial layers (21).

The observed pattern of D₂ and S₂ receptor distribution has at least three important implications for the function of dopamine and serotonin in the mammalian forebrain. First, the sharp lateral-to-medial gradient of D₂ binding in the striatal complex suggests a novel neuro-histochemical basis for the functional distinction between these subregions (22). Second, in view of the high correlation between the potency of antipsychotic drugs in vivo and their affinity for the D₂ binding site (2), the paucity of D₂ sites in the neocortex suggests that a subcortical locus for the action of antipsychotic drugs should be reconsidered. Third, the laminar distribution of S₂ sites in the motor cortex may provide a substrate for the well-documented motor actions of serotonergic compounds acting on brain S₂ sites (23). In addition to permitting quantitative localization of radioligand-labeled receptor subtypes in tissue sections, digital subtraction autoradiography should help to elucidate regional changes in brain receptors related to ontogeny, senescence, or brain injury (4, 25).

C. ANTHONY ALTAR*
STEPHEN O'NEIL

Department of Psychobiology,
University of California, Irvine 92717

ROBERT J. WALTER, JR.
Department of Developmental and
Cellular Biology, University of
California, Irvine

JOHN F. MARSHALL†
Department of Psychobiology,
University of California, Irvine

References and Notes

- O. Hornykiewicz, *Fed. Proc. Fed. Am. Soc. Exp. Biol.* **32**, 183 (1973); A. Carlsson, *Psychol. Med.* **7**, 583 (1977); S. H. Snyder, S. P. Banerjee, H. I. Yamamura, D. Greenberg, *Science* **184**, 1243 (1974); T. J. Crow, E. C. Johnstone, A. Longden, F. Owen, *Adv. Biochem. Pharmacol.* **19**, 301 (1978); J. N. Joyce, *Neurosci. Biobehav. Rev.* **7**, 227 (1983); B. Costall and R. J. Naylor, in *The Neurobiology of Dopamine*, A. S. Horn, Ed. (Academic Press, London, 1979), p. 555.
- S. H. Snyder and R. R. Goodman, *J. Neurochem.* **35**, 5 (1980); P. Seeman, *Pharmacol. Rev.* **32**, 229 (1980); I. Creese, D. R. Sibley, M. W. Hamblin, S. E. Leff, *Annu. Rev. Neurosci.* **6**, 43 (1983).
- J. M. Palacios, D. L. Niehoff, M. J. Kuhar, *Brain Res.* **213**, 277 (1981).
- K. A. Neve, C. A. Altar, C. A. Wong, J. F. Marshall, *ibid.* **302**, 9 (1984).
- I. Creese, R. Schneider, S. H. Snyder, *Eur. J. Pharmacol.* **46**, 377 (1977); I. Creese and S. H. Snyder, *ibid.* **49**, 201 (1978); J. E. Leysen, C. J. E. Niemegeers, J. P. Tollenaere, P. M. Laduron, *Nature (London)* **272**, 168 (1978); N. W. Pedigo, T. D. Reisine, J. Z. Fields, H. I. Yamamura, *Eur. J. Pharmacol.* **50**, 451 (1978); S. J. Peroutka and S. H. Snyder, *Mol. Pharmacol.* **16**, 687 (1979).
- M. Quick, L. L. Iversen, A. Larder, A. V. P. Mackay, *Nature (London)* **274**, 513 (1978).
- J. F. R. König and R. A. Klippel, *The Rat Brain: A Stereotaxic Atlas* (Krieger, New York, 1963).
- Tissue derived from 2- to 4-month-old male Sprague-Dawley albino rats was incubated in 50 mM Tris containing 120 mM NaCl, 5 mM KCl, 2 mM CaCl₂, 1 mM MgCl₂, and 0.01 percent ascorbate. Binding of [³H]spiroperidol to the D₂ sites reached equilibrium by 30 minutes (4). Rinse parameters were determined to optimize dissociation of the nonspecifically bound radioligand. All coronal brain sections that were incubated with a displacer compound were situated 20 to 80 μm from the section incubated with [³H]spiroperidol only.
- P. Jenner and C. D. Marsden, *Neuropharmacology* **20**, 1285 (1981).
- D. R. Howlett and S. R. Nahorski, *Life Sci.* **26**, 511 (1980).
- S. J. List and P. Seeman, *Proc. Natl. Acad. Sci. U.S.A.* **78**, 2620 (1981).
- J. E. Leysen *et al.*, *Life Sci.* **28**, 1015 (1981).
- J. E. Leysen, C. J. E. Niemegeers, J. M. Van Nueten, P. M. Laduron, *Mol. Pharmacol.* **21**, 30 (1982).
- D. Marchais, J. P. Tassin, J. Bockaert, *Brain Res.* **183**, 235 (1980).
- C. A. Altar, R. J. Walter, Jr., K. A. Neve, J. F. Marshall, *J. Neurosci. Methods* **10**, 173 (1984).
- Saturation analysis of 1 μM (+)-butaclamol-displaced [³H]spiroperidol (0.15 to 2.1 nM) binding from developed autoradiographs revealed the following dissociation constant (K_d) and maximum binding (B_{max}) values: caudate-putamen, 0.23 nM and 4590 fmol per milligram of protein; nucleus accumbens, 0.32 and 3600; olfactory tubercle, 0.16 and 3110; layer 5A of motor cortex, 1.54 and 2840; and claustrum, 1.86 and 4520. Differences in the efficiency of tritium penetration through gray and white matter [G. M. Alexander, R. J. Schwartzman, R. D. Bell, J. Yu, A. Renthal, *Brain Res.* **223**, 59 (1981); M. Herkenham and L. Sokoloff, *Soc. Neurosci. Abstr.* **9**, 329 (1983)] as well as a time-dependent loss of [³H]formaldehyde from tissue standards may result in errors in estimating [³H]spiroperidol binding to brain regions. These considerations may affect B_{max} values but do not affect calculated K_d values or the results from displacement curves (Fig. 2), for which tritiated ligand concentration is expressed as a percentage of concentration in the same structure in neighboring sections.
- Concentrations of ketanserin in excess of 100 nM resulted in a slight further displacement that was not regionally selective. This and other research [J. Marcusson, D. G. Morgan, B. Winblad, C. E. Finch, *Soc. Neurosci. Abstr.* **9**, 216 (1983)] indicates that, above 100 nM, ketanserin displaces [³H]spiroperidol from a non-D₂, non-S₂ site. The extent of [³H]spiroperidol binding to α₁ receptor sites was determined with prazosin (12). In concentrations up to 200 nM, prazosin failed to displace [³H]spiroperidol from any of the brain regions examined.
- M. Quik and L. L. Iversen, *Eur. J. Pharmacol.* **56**, 323 (1979).
- E. W. Boehme and R. D. Ciaranello, *Proc. Natl. Acad. Sci. U.S.A.* **78**, 3255 (1981); S. L. Lazareno and S. R. Nahorski, *Eur. J. Pharmacol.* **81**, 273 (1982).
- P. Redgrave and I. Mitchell, *Neuroscience* **7**, 871 (1982); T. DiPaolo, M. Daigle, A. DuPont, *Can. J. Neurol. Sci.* **9**, 421 (1982); J. N. Joyce, S. Loesch, J. F. Marshall, *Brain Res.*, in press.
- H. G. W. Lidov, R. Grazanna, M. E. Molliver, *Neuroscience* **5**, 207 (1980); Y. Takeuchi, H. Kimura, T. Matsuura, T. Yonezawa, Y. Sano, *J. Histochem. Cytochem.* **31**, 181 (1983).
- I. Divac and N. H. Diemer, *J. Comp. Neurol.* **190**, 1 (1980).
- S. J. Peroutka, R. M. Lebovitz, S. H. Snyder, *Science* **212**, 827 (1981).
- M. M. Bradford, *Anal. Biochem.* **72**, 248 (1976).
- The image analysis system is part of the LAMP facility at the University of California, Irvine. This research was supported by NSF grant BNS 8208656, PHS grants NS 20122 and AG 00538 to J.F.M., and by PHS postdoctoral training grant AG00096 to C.A.A. We thank H. Killackey for advice concerning cortical distribution and D. Aswad, M. Baudry, M. Leon, and P. Yahr for comments on the manuscript.

* Present address: Neuroscience Research, Pharmaceuticals Division, CIBA-Geigy Corp., Summit, N.J. 07901.

† To whom requests for reprints should be sent.

14 June 1984; 26 October 1984

Regenerating Fish Optic Nerves and a Regeneration-Like Response in Injured Optic Nerves of Adult Rabbits

Abstract. *Regeneration of fish optic nerve (representing regenerative central nervous system) was accompanied by increased activity of regeneration-triggering factors produced by nonneuronal cells. A graft of regenerating fish optic nerve, or a "wrap-around" implant containing medium conditioned by it, induced a response associated with regeneration in injured optic nerves of adult rabbits (representing a nonregenerative central nervous system). This response was manifested by an increase of general protein synthesis and of selective polypeptides in the retinas and by the ability of the retina to sprout in culture.*

The central nervous system (CNS) of higher vertebrates, unlike that of lower vertebrates, is not capable of posttraumatic regeneration (1-4). Injury in CNS of lower vertebrates alters synthesis and transport of selective molecules (5-10) and sprouting activity in culture (11, 12). The lack of posttraumatic regenerative

response in mammals could stem either from the intrinsic inability of the cell body to undergo the appropriate changes or from a deficient or hostile environment. Indeed, in a nonregenerative CNS, environmental modifications can induce morphological regeneration (13, 14). In regenerative systems, axonal in-